

Quantitatively improved finite-size criteria for spectral gaps

Marius Lemm¹ and David Xiang²

¹*Department of Mathematics, University of Tübingen, 72076 Tübingen, Germany*

²*Harvard College, University Hall, Cambridge, MA 02138, USA*

December 14, 2021

Abstract

Finite-size criteria have emerged as an effective tool for deriving spectral gaps in higher-dimensional frustration-free quantum spin systems. We quantitatively improve the existing finite-size criteria by introducing a novel subsystem weighting scheme. The approach applies to Euclidean lattices of any dimension, the honeycomb lattice, and the triangular lattice.

1 Introduction

In quantum lattice systems, the existence of a spectral gap above the ground state sector places strong constraints on the system's low-energy behavior. For instance, a spectral gap controls ground state correlation in various sense [4, 5, 10, 20] and is central to the classification of topological quantum phases [6, 11]. However, the derivation of a spectral gap is often challenging because excitation energies over the entire Hilbert space need to be controlled. In the better-behaved class of frustration-free quantum spin systems, excitation energies are strictly local and so analytical tools for deriving gaps are available. The list of techniques includes the martingale method [19] and finite-size criteria, which come in two main flavors: those studying the angle between subspaces based on a duality lemma of Fannes-Nachtergaele-Werner [8], see also [24], and those distilled by Knabe [12] from the highly influential work of Affleck-Kennedy-Lieb-Tasaki on their eponymous spin chain [2].

Starting with the work of Gosset-Mozgunov [9], finite-size criteria have seen considerable progress in the last years, especially in the context of higher-dimensional quantum spin systems. This progress concerns both the methodological side [3, 15, 16] and the applications side [1, 13, 14, 17, 18, 21, 22, 23, 25]. Recent methodological advances have mostly focused on the scaling of the gap threshold (called t_ℓ in Eq. (2.1) below) in ℓ , which is of essential theoretical importance. Less attention has been placed on producing thresholds with good constants. This can be a limiting factor when attempting the verification of a finite-size criterion in practice by an explicit calculation of the gap of a particular subsystem. *The main goal of the present paper is to remedy this situation by substantially improving the constants entering the threshold t_ℓ .*

Our first main result concerns the gap thresholds on the Euclidean lattice in any dimension and is formally stated in Theorem 2.2 below. Our main contribution is a new weighting scheme which has the benefit of adapting seamlessly to dimensions ≥ 3 where deriving the optimal threshold scaling ℓ^{-2} has so far been inaccessible to the weighting approach of [9] and instead required sophisticated tools from quantum information theory [3]. The heuristic idea underlying our weighting scheme is that tensor-like product structures allow for computationally efficient and dimensionally robust

encodings of the weighting scheme, while at the same time allowing to effectively implement the principle that the weight of an interaction term should increase with its distance to the boundary of the subsystem.

We also provide finite-size criteria for the honeycomb and triangular lattices in Theorems 2.5 and 2.7 respectively. For both of these lattices, we obtain for the first time the optimal inverse-square threshold scaling ℓ^{-2} which should be sharp in view of the excitation energy of spin wave trial states for the ferromagnetic Heisenberg Hamiltonians on these respective graphs.

2 Setup and main results

Consider a quantum spin system in which one qudit \mathbb{C}^d is placed at each site of the box

$$\Lambda_L = ([0, L] \cap \mathbb{Z})^d$$

so the total Hilbert space of the system is $\bigotimes_{x \in \Lambda_L} \mathbb{C}^d$. On it, we consider a Hamiltonian with nearest-neighbor interactions,

$$H_L^{\text{per}} = \sum_{x \in \Lambda_L} \sum_{1 \leq j \leq D} h_{x, e_j}$$

and with periodic boundary conditions. The local interaction is given by

$$h_{x, e_j} = h \otimes \text{Id}_{\Lambda_L \setminus \{x, x+e_j\}}$$

for a fixed projector $h : \mathbb{C}^d \otimes \mathbb{C}^d \rightarrow \mathbb{C}^d \otimes \mathbb{C}^d$. Note that the edges are directed and the local interaction h_{x, e_j} is allowed to depend on the orientation of the edge. The fact that h is identical across Λ_L makes H_L a translation-invariant Hamiltonian.

Assumption 2.1. H_{Λ_L} is frustration-free for every $L \geq 1$, i.e., $\inf \text{spec } H_{\Lambda_L} = 0$.

We recall that there exist many physically relevant example of frustration-free Hamiltonians, e.g., ferromagnetic Heisenberg models, AKLT models, and Motzkin spin chains. We denote by γ_L^{per} the spectral gap of H , which by frustration-freeness equals the smallest positive eigenvalue of H_{Λ_L} , i.e.,

$$\gamma_L^{\text{per}} = \inf (\text{spec } H_{\Lambda_L} \setminus \{0\}).$$

For $\ell \geq 1$, we similarly define the Hamiltonian

$$H_{\Lambda_\ell} = \sum_{x \in \Lambda_\ell} \sum_{1 \leq j \leq D} h_{x, e_j}$$

with open boundary conditions and we denote its spectral gap by γ_ℓ . Note that Assumption 2.1 ensures that H_{Λ_ℓ} is frustration-free as well.

2.1 Finite-size criteria on Euclidean lattices

We briefly recall the existing finite-size criteria on Euclidean (or hypercubic) lattices of spatial dimension D and state our main result. We consider finite-size criteria of the generic form

$$\gamma_L^{\text{per}} \geq c_\ell (\gamma_\ell - t_\ell) \tag{2.1}$$

with L sufficiently large compared to ℓ . In practice, this can be applied as follows: If there exists a small system size ℓ such that by an explicit calculation one can show $\gamma_\ell > t_\ell$, then one obtains

$\gamma_L^{\text{per}} \geq c > 0$ with c independent of L , i.e., a gap in the infinite-volume limit. We see that the constant c_ℓ is largely irrelevant for the intended use of the criterion. By contrast, the numerical value of the so-called *local gap threshold* t_ℓ is absolutely critical.

Finite-size criteria of the form (2.1) with the following thresholds t_ℓ have been derived.

- Knabe [12] proved (2.1) in one dimension with threshold $t_\ell = \frac{1}{\ell}$.
- Gosset-Mozgunov [9] proved (2.1) in one dimension with $t_\ell = \frac{6}{(\ell+1)(\ell+2)} \sim \frac{6}{\ell^2}$ for ℓ large and in two dimensions with threshold $t_\ell = \frac{8}{\ell^2}$ for slightly modified regions. See [16] for a related result for open boundary conditions.
- [15] proved (2.1) in any dimension with threshold $t_\ell = \frac{3}{\ell}$.
- Anshu [3] proved (2.1) in any dimension with threshold $t_\ell = \frac{D^2 6^D 800(4D-2)^2}{\ell^2}$.

Here, “dimension” always refers to the spatial dimension D . The local Hilbert space dimension d can be arbitrary. Regarding conventions, we note that in the present paper, we use the convention that ℓ counts the number of bonds along each side of Λ_ℓ ; this is 1 less than the number of sites which is used in some of the works mentioned above.

There exist bounds on the best possible threshold asymptotic as $\ell \rightarrow \infty$. Namely, the spin-1/2 Heisenberg ferromagnet on the Euclidean lattice has spectral gap upper bounded by $1 - \cos(\pi/\ell) \sim \frac{\pi^2}{2\ell^2}$ by spin wave theory. This shows that the threshold scaling necessarily satisfies $t_\ell \gtrsim \frac{\pi^2}{2\ell^2} \approx \frac{4.93}{\ell^2}$ as $\ell \rightarrow \infty$ in any dimension. In particular, the inverse-square behavior of t_ℓ that has been found is optimal.

Our first main result reads as follows.

Theorem 2.2 (Main result on Euclidean lattices). *Assume that H_{Λ_L} is frustration-free. Let $D \geq 2$ and let $L \geq 5$, $2 \leq \ell < L/2$. Then,*

$$\gamma_L^{\text{per}} \geq \left(\frac{5}{6}\right)^D (\gamma_\ell - t_\ell) \quad (2.2)$$

where

$$t_\ell = \left(\frac{6}{5}\right)^D \left(\frac{5}{\ell^2} + \frac{300}{\ell^3}\right), \quad \ell \geq 10. \quad (2.3)$$

For $2 \leq \ell \leq 9$, the values of t_ℓ are displayed in Table 1 for $D = 2$ and in Table 2 for $D = 3$.

ℓ	2	3	4	5	6	7	8	9
t_ℓ	0.667	0.395	0.257	0.181	0.134	0.104	0.082	0.067
$\ell^2 t_\ell$	2.667	3.547	4.102	4.503	4.808	5.049	5.245	5.407

Table 1: Values of t_ℓ for $D = 2$ and $2 \leq \ell \leq 9$.

Remark 2.3. (i) In formula (2.2) for the threshold t_ℓ , we took care to obtain the best leading asymptotic afforded by the proof method, namely $\left(\frac{6}{5}\right)^D 5\ell^{-2}$. By contrast, the error term is influenced by various choices made in the proof about how to precisely implement error estimates and accordingly depends directly on the minimal ℓ for which the result applies. The above choice of having a formula for t_ℓ valid for all $\ell \geq 10$ with constant 300 in the error term is a compromise between these competing effects.

ℓ	2	3	4	5	6	7	8	9
t_ℓ	.667	0.400	0.264	0.188	0.141	0.110	0.088	0.073
$\ell^2 t_\ell$	2.667	3.593	4.212	4.685	5.061	5.369	5.627	5.846

Table 2: Values of t_ℓ for $D = 3$ and $2 \leq \ell \leq 9$.

- (ii) For fixed small ℓ , the thresholds can be significantly improved by using our procedure but optimizing over parameters well-adapted to the pertinent value of ℓ . For the potential benefit of practitioners interested in applying our refined finite-size criterion to concrete systems, these significantly better thresholds for $2 \leq \ell \leq 9$ are recorded separately in Tables 1 and 2. Analogs of Tables 1 and 2 in dimensions $D \geq 4$ can also be computed by implementing the procedure laid out in the proof of Theorem 2.2.
- (iii) In dimensions $D \geq 3$, the quantitative improvement afforded by Theorem 2.2 over existing thresholds that were reviewed above is substantial. Also in 2D, we obtain a slight asymptotic improvement over the best previously known threshold which satisfies $\ell^2 t_\ell = 8$ [9]. We obtain $\ell^2 t_\ell \sim \frac{36}{5} = 7.2$ as $\ell \rightarrow \infty$. As the example of the Heisenberg ferromagnet shows, one cannot do better than $\ell^2 t_\ell \geq \frac{\pi^2}{2} \approx 4.93$ for ℓ large, so the room for further asymptotic improvements in 2D is limited.

2.2 Discussion

To place this result in context, we first recall that the work [9] introduced a refinement of Knabe’s approach via subsystem Hamiltonians [12] by suitably weighting the local interactions. The weighting scheme used in [9] works well in the two-dimensional setting considered there, but has so far resisted extension to dimensions > 2 for technical reasons. By contrast, [3] proceeds completely differently in higher dimensions via an ingenious use of gap amplification and the detectability lemma from quantum information theory. Until now, [3] was the only proof of the optimal threshold scaling $t_\ell \sim \ell^{-2}$ in higher dimensions. A disadvantage of the detectability lemma approach is that it comes at the price of relatively large constants which can create difficulties in concrete applications where quantitative values matter. It has therefore been of practical interest to find a way to adapt the weighting method to higher dimensions.

The present work shows that the weighting method can be modified to apply in higher dimensions. Our main contribution is to develop a novel weighting scheme which extends to higher dimensions. The main idea is to define the weights through a certain tensor-like product structure; see (3.1) as well as Figures 3 and 4. Implementing this scheme yields the first proof of the optimal threshold scaling in higher dimensions that does not require the detectability lemma. The weighting scheme efficiently implements the general principle that boundary interactions receive lower weights. As a result, our finite-size criterion has the smallest thresholds t_ℓ that are available in the literature, which makes it easier to verify in concrete applications.

We close the discussion by listing possible extensions and an open problem.

Remark 2.4. (i) The assumption that h is a projector is mild. If h is not a projector, we may scale it appropriately and then replace it with a projector onto the orthogonal complement of $\ker h$. The spectral gap of the new Hamiltonian differs only by a constant multiplicative factor from the old Hamiltonian.

- (ii) The proof also applies if the assumptions of rotation- and/or translation-invariance on the interaction are removed. The result is a modified finite-size criterion in which different rotations

and/or translations of subsystems enter on the right-hand side.

- (iii) It is an open problem, though one of purely theoretical nature, whether the threshold scaling $t_\ell \sim \ell^{-2}$ can be derived with dimension-independent constant as was possible for ℓ^{-1} -scaling [15].

2.3 Finite-size criterion for the honeycomb lattice

Motivated by the AKLT conjecture that the honeycomb AKLT model exhibits a spectral gap [2], Knabe investigated a finite-size criterion on the honeycomb lattice already in 1988 [12], albeit inconclusively. Recent years have seen a number of applications of finite-size criteria to the honeycomb and decorated honeycomb lattices [1, 18, 22, 23], in some cases combine with extensive numerical calculations. Here we derive for the first time a general finite-size criterion of the form (2.1) for the honeycomb lattice which has the expected inverse-square threshold scaling just like the Euclidean case studied in Theorem 2.2 but naturally with different constants.

To formulate the result, we let \mathbb{H}_L denote the hexagonal lattice wrapped on an $L \times L$ torus. We write

$$H_{\mathbb{H}_L}^{\text{per}} = \sum_{\substack{x,y \in \mathbb{H}_L \\ x \sim y}} h_{x,y}$$

for the associated Hamiltonian. Since there is no natural orientation of the edges, we assume that the local interaction commutes with the swap operator defined by $S(|\psi\rangle \otimes |\phi\rangle) = (|\phi\rangle \otimes |\psi\rangle)$. We assume that $H_{\mathbb{H}_L}^{\text{per}}$ is frustration-free and write γ_L^{per} for its spectral gap.

The relevant finite subsystems are $\ell \times \ell$ “slanted” grids of hexagons called \mathcal{B}_ℓ as depicted in Figure 1 below. The associated Hamiltonians are denoted by $H_{\mathcal{B}_\ell}$ with spectral gaps γ_ℓ .

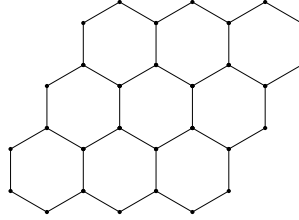


Figure 1: The slanted grid \mathcal{B}_ℓ with $\ell = 3$.

The finite-size criterion on the honeycomb lattice then reads as follows.

Theorem 2.5 (Main result on the honeycomb lattice). *Let $\ell \geq 3, L > 2\ell$. Then,*

$$\gamma_L^{\text{per}} \geq \frac{1}{2}(\gamma_\ell - t_\ell) \tag{2.4}$$

where

$$t_\ell = \frac{228}{55\ell^2} + \frac{108}{\ell^3}, \quad \ell \geq 10. \tag{2.5}$$

For $3 \leq \ell \leq 9$, the thresholds t_ℓ are displayed in Table 4.

Remark 2.6. (i) Analogously to the discussion in Remark 2.3 (i), the restriction to $\ell \geq 10$ arises from a desire to have a reasonable constant in the error term (here 108), while the numbers obtained for $3 \leq \ell \leq 9$ arise through a more targeted optimization procedure of the parameters chosen to define the weighting scheme in the proof.

ℓ	3	4	5	6	7	8	9
t_ℓ	0.246	0.161	0.113	0.084	0.065	0.051	0.042
$\ell^2 t_\ell$	2.212	2.576	2.824	3.003	3.140	3.247	3.333

Table 3: Thresholds t_ℓ on the honeycomb lattice for small values of ℓ .

- (ii) Concerning the best possible threshold on the honeycomb lattice, we can again consider spin wave trial states in the Heisenberg ferromagnet. We performed numerics that then predict a gap scaling $\approx \frac{0.9}{\ell^2}$ which, if sharp, would leave the possibility of further improvement of the constant $\frac{228}{55}$.

2.4 Finite-size criterion for the triangular lattice

We obtain an analogous result for the triangular lattice. We let \mathbb{T}_L denote the triangular lattice wrapped on an $L \times L$ torus and write $H_{\mathbb{T}_L}^{\text{per}}$ for the associated Hamiltonian, which we assume to be frustration-free, and γ_L^{per} for its spectral gap. The relevant finite subsystems are $\ell \times \ell$ “slanted” grids of triangles as shown in Figure 2. The associated subsystem Hamiltonians are denoted by $H_{\mathcal{B}_\ell}$ with gaps γ_ℓ .

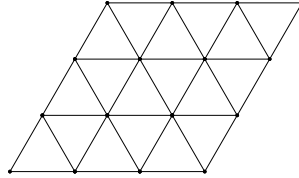


Figure 2: The slanted triangular grid \mathcal{B}_ℓ with $\ell = 3$.

The finite-size criterion on the triangular lattice then reads as follows.

Theorem 2.7 (Main result on triangular lattice). *Let $\ell \geq 3, L > 2\ell$. Then,*

$$\gamma_L^{\text{per}} \geq \frac{1}{2} (\gamma_\ell - t_\ell). \quad (2.6)$$

where

$$t_\ell = \frac{144}{5\ell^2} + \frac{432}{\ell^3}, \quad \ell \geq 10. \quad (2.7)$$

For $3 \leq \ell \leq 9$, the thresholds t_ℓ are displayed in Table 4.

ℓ	3	4	5	6	7	8	9
t_ℓ	1.318	0.872	0.628	0.476	0.373	0.301	0.248
$\ell^2 t_\ell$	11.861	13.946	15.700	17.113	18.263	19.213	20.010

Table 4: Thresholds for the finite-size criterion on the triangular lattice for small values of ℓ .

We remark that it is no coincidence that the constants appearing in Theorem 2.7 are comparatively worse than in the previous two theorems. The underlying reason is that the triangular lattice

has a relatively large number of bonds incident at each site and thus has a large number of locally competing interactions. This makes it comparatively difficult to control the sum of anticommutators corresponding to adjacent edges that arise in the proof from squaring the weighted Hamiltonian. As a benchmark for assessing the sharpness of the finite-size criterion, we note using spin wave trial states for the ferromagnetic Heisenberg model with $S = \frac{1}{2}$ together with numerical computation of eigenvalues of the discrete Laplacian suggest a gap scaling of $\frac{5.3}{\ell^2}$ for large ℓ , which, if sharp, would still leave room for improvement of the constant $\frac{144}{5}$ that we find on the triangular lattice.

3 Proof of Theorem 2.2 on Euclidean lattices

3.1 Construction of weighted subsystem Hamiltonians

Let $D \geq 2$. We will establish (2.2) by studying weighted Hamiltonians on \mathcal{B}_ℓ . This is inspired by the approach of [9], though, the weighting scheme is completely different here. The weighted Hamiltonian $W_{\mathcal{B}_\ell}$, is defined as follows. We use two families of coefficients $c_0, \dots, c_{\ell-1}$ and d_0, \dots, d_ℓ (to be further specified later) satisfying the following requirements:

- (i) The c_i and d_i are positive.
- (ii) The c_i , and d_i are symmetric around the midpoint, i.e., $c_i = c_{\ell-1-i}$ and $d_i = d_{\ell-i}$.
- (iii) The c_i and d_i are increasing up to the midpoint. That is, $c_i \leq c_{i+1}$ for $0 \leq i \leq \lfloor \frac{\ell-1}{2} \rfloor$, and $d_i \leq d_{i+1}$ for $0 \leq i \leq \lfloor \frac{\ell}{2} \rfloor$.

Then, we define the weighted subsystem Hamiltonians as

$$W_{\mathcal{B}_\ell} = \sum_{1 \leq j \leq D} \sum_{\substack{x \in \mathcal{B}_\ell: \\ 0 \leq x_j \leq \ell-1}} c_{x_j} \left(\prod_{\substack{1 \leq k \leq D: \\ k \neq j}} d_{x_k} \right) h_{x, e_j}. \quad (3.1)$$

Note that these subsystem Hamiltonians have open boundary conditions.

Figure 3 depicts the distribution of edge weights that create $W_{\mathcal{B}_3}$ in two dimensions. Notice that conditions (i)-(iii) imply that $c_0 = c_2 \leq c_1$ and $d_0 = d_3 \leq d_1 = d_2$, so our weighting scheme implements the general principle that having large edge weights near the center and comparatively smaller edge weights near the boundary leads to the best thresholds. (This principle can be heuristically understood from the proof of the finite-size criterion leads where the goal is to efficiently cover the lattice through translates of $W_{\mathcal{B}_3}$.) The particular scheme that we propose in (3.1) turns out to implement this general principle in a very efficient manner that allows for convenient calculation especially in higher dimensions.

To understand the product nature of the scheme, observe that the two-dimensional $W_{\mathcal{B}_3}$ depicted in Figure 3 arises as the Hadamard (pointwise) product from two simpler weighted Hamiltonians displayed in Figure 4. This idea of using products as simpler building blocks for realizing (3.1) extends well to higher dimensions. Then the independence-like properties of products are what underlies the calculational convenience of this weighting scheme in higher dimensions. To summarize, formula (3.1) is the key theoretical underpinning of the improved thresholds.

These weighted Hamiltonians will be used to prove the following general gap bound.

Proposition 3.1 (General gap bound on the Euclidean lattice). *For $\ell \geq 2$, let the coefficients $c_0, \dots, c_{\ell-1}$ and d_0, \dots, d_ℓ satisfy requirements (i)-(iii) above. Under the assumptions of Theorem*

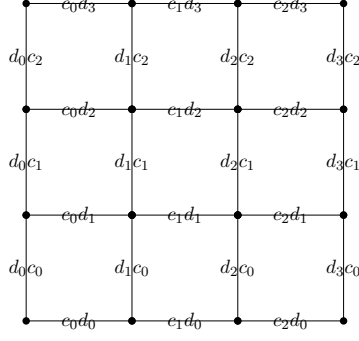


Figure 3: The weighted subsystem Hamiltonian $W_{\mathcal{B}_3}$ on the 2D square grid. Edges are labeled by their weights. Notice that edges in the center have a comparatively higher weight compared to edges along the boundary, which in turn have a relatively higher weight compared to edges at a corner.

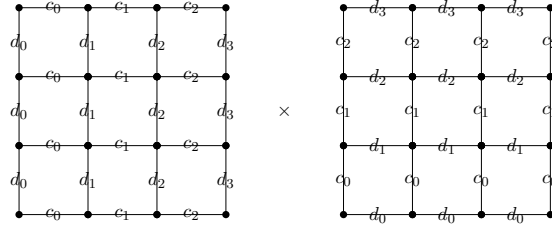


Figure 4: The weighted subsystem Hamiltonian $W_{\mathcal{B}_3}$ displayed in Figure 3 arises as the pointwise product of these two simpler weighting schemes.

2.2, we have

$$\gamma_L^{\text{per}} \geq \frac{K_4}{K_3} \left(\gamma_\ell - \frac{K_0 + K_3 - 2K_1}{K_4} \right), \quad (3.2)$$

provided that $K_3 \geq \max\{K_1, K_2\}$, where we introduced the effective constants

$$\begin{aligned} K_0 &= \left(\sum_{i=0}^{\ell-1} c_i^2 \right) \left(\sum_{i=0}^{\ell} d_i^2 \right)^{D-1} \\ K_1 &= \left(\sum_{i=0}^{\ell-1} c_i^2 \right) \left(\sum_{i=0}^{\ell-1} d_i d_{i+1} \right) \left(\sum_{i=0}^{\ell} d_i^2 \right)^{D-2} \\ K_2 &= \left(\sum_{i=0}^{\ell-2} c_i c_{i+1} \right) \left(\sum_{i=0}^{\ell} d_i^2 \right)^{D-1} \\ K_3 &= \left(\sum_{i=0}^{\ell-1} c_i d_i \right)^2 \left(\sum_{i=0}^{\ell} d_i^2 \right)^{D-2} \\ K_4 &= \frac{1}{\ell(\ell+1)^{D-1}} \left(\sum_{i=0}^{\ell-1} c_i \right)^2 \left(\sum_{i=0}^{\ell} d_i \right)^{2(D-1)}. \end{aligned} \quad (3.3)$$

In the next few subsections, we prove Proposition 3.1. Afterwards, in Subsections 3.6 and 3.7, we discuss how to choose the parameters c_i and d_i to optimize the local gap threshold $\frac{K_0 + K_3 - 2K_1}{K_4}$.

which will complete the proof of Theorem 2.2.

3.2 Expansion of the auxiliary operator

For every site $t \in \Lambda_L$, we can define the translated box

$$B_t = \{x \in \Lambda_L : x - t \in \mathcal{B}_\ell\}$$

Recall that we use periodic boundary conditions on Λ_L but open boundary conditions on B_ℓ . We denote the corresponding unweighted and weighted Hamiltonians (the latter defined analogously to (3.1)) by H_{B_t} and W_{B_t} , respectively, which can be obtained by conjugating $H_{\mathcal{B}_\ell}, W_{\mathcal{B}_\ell}$ with translation. Since translation is unitary, the spectral gap is independent of t . We consider the auxiliary operator $A = \sum_{t \in \Lambda_L} W_{B_t}^2$. This operator can be written as a weighted sum of anti-commutators $\{h_{x,e_j}, h_{y,e_k}\} = h_{x,e_j} h_{y,e_k} + h_{y,e_k} h_{x,e_j}$, i.e.

$$A = \sum_{t \in \Lambda_L} W_{B_t}^2 = \sum_{(x,j) \in \Lambda_L \times [D]} w_{x,j} h_{x,e_j}^2 + \sum_{\substack{(x,j), (y,k) \in \Lambda_L \times [D]: \\ (x,e_k) \neq (y,e_k)}} w_{x,y,j,k} \{h_{x,e_j}, h_{y,e_k}\}. \quad (3.4)$$

where we denoted $[D] = \{1, \dots, D\}$ for appropriate effective weights $w_{x,j}$ and $w_{x,y,j,k}$ to be investigated in the following. Computing these coefficient will lead us to the explicit formula (3.7) below.

First, we have

$$w_{x,j} = \left(\sum_{i=0}^{\ell-1} c_i^2 \right) \left(\sum_{i=0}^{\ell} d_i^2 \right)^{D-1} = K_0$$

Combining this with the fact that $h_{x,e_j}^2 = h_{x,e_j}$ (since the h_{x,e_j} are projectors) we find

$$\sum_{(x,e_j) \in \Lambda_L \times [D]} w_{x,j} h_{x,e_j}^2 = K_0 H_{\Lambda_L},$$

which is the first term in (3.7).

Next, we consider the off-diagonal weights $w_{x,y,j,k}$ in (3.4). We write $x = (x_1, \dots, x_d), y = (y_1, \dots, y_d)$ and $z_j = |x_j - y_j|$.

Case $j = k$. This means that the two relevant edges are collinear. Then,

$$w_{x,y,j,j} = \left(\sum_{i=0}^{\ell-1-z_j} c_i c_{i+z_j} \right) \prod_{\substack{2 \leq m \leq D: \\ m \neq j}} \left(\sum_{j=0}^{\ell-z_m} d_j d_{j+z_m} \right) \quad (3.5)$$

Here, we use the assumption that $L > 2\ell$, as otherwise one might have terms such as $d_i d_{i+\ell-z_m}$ in the sums. We claim the expressions $\sum_{i=0}^{\ell-1-z_j} c_i c_{i+z_j}$ and $\sum_{j=0}^{\ell-z_m} d_j d_{j+z_m}$ are monotonically decreasing in the distances z_1, \dots, z_D under our assumptions on c_i, d_i . To see this, suppose we choose $a_i, b_i, 0 \leq i \leq n$, such that the $a_i = 1_{i \in [j, \ell-j]}, b_i = 1_{i \in [k, n-k]}$. Then $\sum_{i=0}^{\ell-z_m} a_i b_{i+z_m}$ is decreasing in z_k , and then linearity shows that $\sum_{i=0}^{\ell-z_k} d_i d_{i+z_k}$ is decreasing in z_k . An identical argument holds for the c_i .

Since $x \neq y$, we have $\sum_{1 \leq m \leq D} z_m \geq 1$ which is minimal for $\sum_{1 \leq m \leq D} z_m \geq 1 = 1$. In other words, the maximum value of $w_{x,y,j,j}$ when x and y are nearest neighbors. There are two possibilities for this: (i) both edges are incident to the same vertex, i.e. the edge pair is of the shape $\bullet \rightarrow \bullet$, which translates to $z_j = 1$ and all other $z_m = 0$. (ii) Both edges are parallel but do not overlap at

a vertex, i.e., $y = x + e_{m_0}$ for some $m_0 \neq j$. We represent this case by the edge pair $\overleftrightarrow{\text{---}}$. This case translates to $z_{m_0} = 1$ for some $m_0 \neq j$ and all other $z_m = 0$. Distinguishing these cases in (3.5), we conclude that

$$w_{x,y,j,j} \leq \max\{K_1, K_2\},$$

for the effective constants

$$K_1 = \left(\sum_{i=0}^{\ell-2} c_i c_{i+1} \right) \left(\sum_{i=0}^{\ell} d_i^2 \right)^{D-1}, \quad K_2 = \left(\sum_{i=0}^{\ell-1} c_i^2 \right) \left(\sum_{i=0}^{\ell-1} d_i d_{i+1} \right) \left(\sum_{i=0}^{\ell} d_i^2 \right)^{D-2}.$$

Case $j \neq k$. Without loss of generality, we assume $j = 1, k = 2$, in which case

$$w_{x,y,1,2} = \left(\sum_{i=0}^{\ell-z_1-1} c_i d_{i+z_1} \right) \left(\sum_{i=0}^{\ell-z_2-1} c_i d_{i+z_2} \right) \prod_{k=3}^D \left(\sum_{i=0}^{\ell-z_k} d_i d_{i+z_k} \right).$$

Via a similar argument as before, the above quantity is decreasing in z_1, z_2 , and as a result the maximum value of $w_{x,y,1,2}$ is achieved by adjacent edges of the shape $\overrightarrow{\text{---}}$. This yields the bound

$$w_{x,y,1,2} \leq K_3 = \left(\sum_{i=0}^{\ell-1} c_i d_i \right)^2 \left(\sum_{i=0}^{\ell} d_i^2 \right)^{D-2}, \quad j \neq k. \quad (3.6)$$

The fact that the upper bound is K_3 for all choices of orientation of the edge shape $\overrightarrow{\text{---}}$ follows from the symmetry of the c_i, d_i and relabelling the summation indices appropriately.

Thus, we can expand the second term in (3.4) to obtain

$$A = K_0 H_{\Lambda_L} + K_1 \sum_{\overleftrightarrow{\text{---}}} \{h_{x,e_j}, h_{y,e_k}\} + K_2 \sum_{\overleftrightarrow{\text{---}}} \{h_{x,e_j}, h_{y,e_k}\} + K_3 \sum_{\overrightarrow{\text{---}}} \{h_{x,e_j}, h_{y,e_k}\} + R_A, \quad (3.7)$$

where the sums are over all edge pairs of the indicated type, and R_A consists of the anti-commutators corresponding to all remaining edge pairs. The monotonicity established above and our assumption that $K_3 \geq \max\{K_1, K_2\}$ imply that the positive coefficient of any particular commutator $\{h_{x,e_j}, h_{y,e_k}\}$ in R_G is bounded above by K_3 .

3.3 Comparison to the squared Hamiltonian

We may now similarly expand $H_{\Lambda_L}^2$, writing

$$H_{\Lambda_L}^2 = H_{\Lambda_L} + \sum_{\overleftrightarrow{\text{---}}} \{h_{x,e_j}, h_{y,e_k}\} + \sum_{\overleftrightarrow{\text{---}}} \{h_{x,e_j}, h_{y,e_k}\} + \sum_{\overrightarrow{\text{---}}} \{h_{x,e_j}, h_{y,e_k}\} + R_{\Lambda_L} \quad (3.8)$$

where again R_{Λ_L} contains the anti-commutators corresponding to all remaining edge pairs. Since the edge pairs entering R_{Λ_L} do not share a vertex, the corresponding projections commute and satisfy the positivity $\{h_{x,e_j}, h_{y,e_k}\} \geq 0$. Considering that the coefficient of any particular commutator in R_A is bounded above by K_3 , we conclude that the operator $K_3 R_{\Lambda_L} - R_A$ is a positive linear combination of positive operators. Analogous reasoning yields

$$(K_3 - K_2) \sum_{\overleftrightarrow{\text{---}}} \{h_{x,e_j}, h_{y,e_k}\} \geq 0.$$

Combining these estimates with our expansions (3.7) and (3.8), we obtain the operator inequality

$$K_3 H_{\Lambda_L}^2 - \sum_{l \in \Lambda_L} W_{B_l}^2 \geq (K_3 - K_0) H_{\Lambda_L} + (K_3 - K_1) \sum_{\bullet \text{---} \bullet} \{h_{x,e_j}, h_{y,e_k}\}.$$

To treat the last term, we draw on an idea of [15] and apply the operator Cauchy-Schwarz inequality in the form

$$-\{h_{x,e_j}, h_{y,e_k}\} \leq (-h_{x,e_j})^2 + h_{y,e_k}^2 = h_{x,e_j} + h_{y,e_k}$$

which implies

$$\sum_{\bullet \text{---} \bullet} \{h_{x,e_j}, h_{y,e_k}\} \geq -2H_{\Lambda_L},$$

because each edge is contained in precisely two bond pairs of the shape $\bullet \text{---} \bullet$. We have shown that

$$K_3 H_{\Lambda_L}^2 - \sum_{t \in \Lambda_L} W_{B_t}^2 \geq (2K_1 - K_0 - K_3) H_{\Lambda_L} \quad (3.9)$$

which we point out already bears some similarity with (3.2).

3.4 Translation-invariant excited states

Finally, we compare $\sum_{t \in \Lambda_L} W_{B_t}^2$ with H_{Λ_L} . The naive estimate involving the spectral gap of the unweighted operator times the smallest coefficient $\min\{c_0, d_0\}$ is insufficient. Instead, we use the following refinement which leverages translation-invariance and is directly inspired by [9, Lemma 4].

Lemma 3.2. *There exists a normalized state $|\phi\rangle$ satisfying $H_{\Lambda_L} |\phi\rangle = \gamma_{\Lambda_L}^{\text{per}} |\phi\rangle$ such that*

$$\langle \phi, W_{B_t}^2 \phi \rangle \geq \gamma_\ell \left(\min_{1 \leq j \leq D} \frac{1}{\ell(\ell+1)^{D-1}} \sum_{\substack{x \in B_t \\ 0 \leq x_j \leq \ell-1}} w_{x,e_j} \right) \langle \phi, W_{B_t} \phi \rangle, \quad t \in \Lambda_L. \quad (3.10)$$

Proof of Lemma 3.2. Let T_i be spatial translation in the direction i . Then, since the $\{T_i\}_{1 \leq i \leq D}$ and H_{Λ_L} all mutually commute, we can simultaneously diagonalize these operators. Thus, we can find a state $|\phi\rangle$ lying in the γ_L^{per} -eigenspace of H_{Λ_L} such that $|\phi\rangle$ is also an eigenvector of all the T_i 's. For any two bonds $(x, e_j), (y, e_j)$, by conjugating with the translation operators we find that the energy

$$\langle \phi | h_{x,e_j} | \phi \rangle = \langle \phi | h_{y,e_j} | \phi \rangle \quad (3.11)$$

is constant across all bonds.

Next, let P be the projector onto the ground state of W_{B_t} , and write P^\perp for $I - P$. If $P^\perp |\phi\rangle = 0$ then both sides in (3.10) vanish by frustration-freeness and the claim is trivial. Hence, we may assume $P^\perp |\phi\rangle \neq 0$ and write $|\hat{\phi}\rangle$ for the corresponding normalized state which satisfies $\langle \hat{\phi}, X \hat{\phi} \rangle = \langle \phi, X \phi \rangle \langle \phi, P^\perp \phi \rangle$ for any bounded operator X .

Consider the case $t = 0$, i.e., $B_t = \mathcal{B}_\ell$. From Jensen's inequality

$$\langle \phi, W_{\mathcal{B}_\ell}^2 \phi \rangle = \langle \hat{\phi}, W_{\mathcal{B}_\ell}^2 \hat{\phi} \rangle \langle \phi, P^\perp \phi \rangle \geq (\langle \hat{\phi}, W_{\mathcal{B}_\ell} \hat{\phi} \rangle)^2 \langle \phi, P^\perp \phi \rangle = \langle \hat{\phi}, W_{\mathcal{B}_\ell} \hat{\phi} \rangle \langle \phi, W_{\mathcal{B}_\ell} \phi \rangle.$$

The energy identity (3.11) extends to $|\hat{\phi}\rangle$, i.e., $\langle \hat{\phi} | h_{x,e_j} | \hat{\phi} \rangle = \langle \hat{\phi} | h_{y,e_j} | \hat{\phi} \rangle$ which lets us average over the weights in $W_{\mathcal{B}_\ell}$, i.e.,

$$\begin{aligned}
\langle \hat{\phi}, W_{\mathcal{B}_\ell} \hat{\phi} \rangle &= \left\langle \hat{\phi}, \sum_{1 \leq j \leq D} \sum_{\substack{x \in \mathcal{B}_\ell: \\ 0 \leq x_j \leq \ell-1}} w_{x,e_j} h_{x,e_j} \hat{\phi} \right\rangle \\
&= \left\langle \hat{\phi}, \sum_{1 \leq j \leq D} \sum_{\substack{x \in \mathcal{B}_\ell: \\ 0 \leq x_j \leq \ell-1}} \left(\frac{1}{\ell(\ell+1)^{D-1}} \sum_{\substack{y \in \mathcal{B}_\ell: \\ 0 \leq y_j \leq \ell-1}} w_{y,e_j} \right) h_{x,e_j} \hat{\phi} \right\rangle \\
&\geq \left(\min_{1 \leq j \leq D} \frac{1}{\ell(\ell+1)^{D-1}} \sum_{\substack{y \in \mathcal{B}_\ell: \\ 0 \leq y_j \leq \ell-1}} w_{y,e_j} \right) \langle \hat{\phi} | H_{\mathcal{B}_\ell} | \hat{\phi} \rangle \\
&\geq \gamma_\ell \left(\min_{1 \leq j \leq D} \frac{1}{\ell(\ell+1)^{D-1}} \sum_{\substack{y \in \mathcal{B}_\ell: \\ 0 \leq y_j \leq \ell-1}} w_{y,e_j} \right)
\end{aligned}$$

where in the last step we used the fact that $\hat{\phi}$ has been chosen so that it is orthogonal to the ground state of $W_{\mathcal{B}_\ell}$ and thus also of $H_{\mathcal{B}_\ell}$. (The weights do not change the zero eigenspace since they are positive.) The argument for $t \neq 0$ is analogous. This proves Lemma 3.2. \square

3.5 Proof of Proposition 3.1

We take the expectation value of (3.9) in the normalized state $|\phi\rangle$ whose existence is guaranteed by Lemma 3.2. Using $H_{\Lambda_L} |\phi\rangle = \gamma_{\Lambda_L}^{\text{per}} |\phi\rangle$, we obtain

$$K_3(\gamma_{\Lambda_L}^{\text{per}})^2 - \left\langle \phi, \sum_{t \in \Lambda_L} W_{B_t}^2 \phi \right\rangle \geq (2K_1 - K_0 - K_3) \gamma_{\Lambda_L}^{\text{per}}. \quad (3.12)$$

For our choice of weights, the average $\frac{1}{\ell(\ell+1)^{D-1}} \sum_y w_{y,e_j}$ in (3.10) is independent of direction j . Expressing this average in terms of the coefficients c_i, d_i gives

$$\langle \phi | W_{B_\ell}^2 | \phi \rangle \geq \frac{\gamma_\ell}{\ell(\ell+1)^{D-1}} \left(\sum_{i=0}^{\ell-1} c_i \right) \left(\sum_{i=0}^{\ell} d_i \right)^{D-1} \langle \phi | W_{B_\ell} | \phi \rangle \quad (3.13)$$

The same inequality holds for all translates $W_{B_t}^2$ thanks to translation-invariance. Summing (3.13) over all translates $W_{B_t}^2$, we obtain

$$\begin{aligned}
\sum_{t \in \Lambda_L} \langle \phi | W_{B_t}^2 | \phi \rangle &\geq \frac{\gamma_\ell}{\ell(\ell+1)^{D-1}} \left(\sum_{i=0}^{\ell-1} c_i \right) \left(\sum_{i=0}^{\ell} d_i \right)^{D-1} \left\langle \phi, \sum_{t \in \Lambda_L} W_{B_t} \phi \right\rangle \\
&= \frac{\gamma_\ell}{\ell(\ell+1)^{D-1}} \left(\sum_{i=0}^{\ell-1} c_i \right)^2 \left(\sum_{i=0}^{\ell} d_i \right)^{2(D-1)} \langle \phi, H_{\Lambda_L} \phi \rangle \\
&= \gamma_\ell \gamma_L^{\text{per}} K_4,
\end{aligned}$$

where the second step uses that in the sum $\sum_{t \in \Lambda_L} W_{Bt}$, each projector h_{x,e_j} appears with coefficient $\sum_x w_{x,e_j} = K_0$ and the last step uses that $H_{\Lambda_L}|\phi\rangle = \gamma_{\Lambda_L}^{\text{per}}|\phi\rangle$.

Returning to (3.12) and using that $\gamma_L^{\text{per}} > 0$ by definition, we have shown that

$$\gamma_L^{\text{per}} \geq \frac{K_4}{K_3} \left(\gamma_\ell - \frac{K_0 + K_3 - 2K_1}{K_4} \right) \quad (3.14)$$

which proves Proposition 3.1. \square

3.6 Parameters in 2 dimensions

In this section we consider $D = 2$.

Proof of Theorem 2.2 for $D = 2$. We have Proposition 3.1 for all weights c_i, d_i satisfying requirements (i)-(iii) above. For $D = 2$,

$$\begin{aligned} K_0 &= \left(\sum_{i=0}^{\ell-1} c_i^2 \right) \left(\sum_{i=0}^{\ell} d_i^2 \right), & K_1 &= \left(\sum_{i=0}^{\ell-2} c_i c_{i+1} \right) \left(\sum_{i=0}^{\ell} d_i^2 \right), \\ K_2 &= \left(\sum_{i=0}^{\ell-1} c_i^2 \right) \left(\sum_{i=0}^{\ell-1} d_i d_{i+1} \right), & K_3 &= \left(\sum_{i=0}^{\ell-1} c_i d_i \right)^2, \\ K_4 &= \frac{1}{\ell^2 + \ell} \left(\sum_{i=0}^{\ell-1} c_i \right)^2 \left(\sum_{i=0}^{\ell} d_i \right)^2 \end{aligned}$$

In view of (3.2), the main goal is to choose the coefficients c_i, d_i such that the threshold

$$\frac{K_0 + K_3 - 2K_1}{K_4}$$

is as small as possible.

We set

$$\begin{aligned} c_j &= \ell + (\ell - 1)j - j^2, & \text{for } j = 0, \dots, \ell - 1, \\ d_j &= (1 - \lambda)(\ell + 1 + \ell j - j^2) + \lambda \frac{(\ell + 2)^2}{4}, & \text{for } j = 0, \dots, \ell \end{aligned} \quad (3.15)$$

with interpolation parameter $\lambda = \frac{2(\sqrt{2}-1)}{\ell}$. These satisfy the requirements (i)-(iii) from above.

It remains to explicit calculate the threshold $\frac{K_0 + K_3 - 2K_1}{K_4}$ in terms of the polynomials K_0, K_1, \dots, K_4 and to use various elementary error estimates.

Asymptotics. Before we present the rigorous error estimates, let us check that the result is correct to leading order in ℓ . First, to check the constraint $K_3 \geq K_1, K_2$, we consider

$$\begin{aligned} K_3 - K_1 &= \frac{2 + \sqrt{2}}{360} \ell^7 + \mathcal{O}(\ell^6) \\ K_3 - K_2 &= \frac{5 - 3\sqrt{2}}{360} \ell^7 + \mathcal{O}(\ell^6), \end{aligned} \quad (3.16)$$

which holds asymptotically as $\ell \rightarrow \infty$. We see that for large enough ℓ it will indeed be the case that $K_3 \geq K_1, K_2$. The threshold can be written as

$$\frac{K_0 + K_3 - 2K_1}{K_4} = \frac{(\ell^2 + \ell)(K_0 + K_3 - 2K_1)}{\left(\sum_{i=0}^{\ell-1} c_i \right)^2 \left(\sum_{i=0}^{\ell} d_i \right)^2} \quad (3.17)$$

Here, after cancellations, the numerator is given by a degree 10 polynomial with leading coefficients of the form

$$(\ell^2 + \ell)(K_0 + K_3 - 2K_1) = \frac{1}{180}\ell^{10} + \frac{28 + 3\sqrt{2}}{360}\ell^9 + \mathcal{O}(\ell^{10}). \quad (3.18)$$

The denominator is a degree 12 polynomial with leading coefficients of the form

$$\left(\sum_{i=0}^{\ell-1} c_i\right)^2 \left(\sum_{i=0}^{\ell} d_i\right)^2 = \frac{1}{1296}\ell^{12} + \frac{8 + \sqrt{2}}{648}\ell^{11} + \mathcal{O}(\ell^{10}). \quad (3.19)$$

The asymptotic statements (3.18) and (3.19) already establish that the leading coefficient is as displayed in Theorem 2.2, i.e.,

$$\frac{K_0 + K_3 - 2K_1}{K_4} < \frac{36}{5\ell^2} + \mathcal{O}\left(\frac{1}{\ell^3}\right) \quad (3.20)$$

Error estimates. We now present explicit error estimates that yield the claimed explicit error term in (3.20). First, by explicitly computing all coefficients in (3.16), one can establish $K_3 \geq K_1, K_2$ as soon as $\ell \geq 3$.

Furthermore, through various elementary estimates we obtain the following precise versions of (3.18) and (3.19),

$$(\ell^2 + \ell)(K_0 + K_1 - 2K_3) < \frac{1}{180}\ell^{10} + \frac{1}{5}\ell^9, \quad \ell \geq 10,$$

and

$$\left(\sum_{i=0}^{\ell-1} c_i\right)^2 \left(\sum_{i=0}^{\ell} d_i\right)^2 > \frac{1}{1296}\ell^{12}, \quad \ell \geq 10.$$

This allows to estimate the threshold by

$$\frac{K_0 + K_3 - 2K_1}{K_4} < \frac{36}{5\ell^2} + \frac{1296}{5\ell^3}, \quad \ell \geq 10.$$

We recall Proposition 3.1 and use

$$\frac{K_4}{K_3} \geq \frac{25}{36}, \quad \ell \geq 10.$$

to obtain

$$\gamma_L^{\text{per}} \geq \frac{25}{36} \left(\gamma_\ell - \frac{36}{5\ell^2} - \frac{1296}{5\ell^3} \right), \quad \ell \geq 10, \quad (3.21)$$

which proves Theorem 2.2 for $D = 2$. \square

Let us briefly discuss the heuristics underlying the choice of coefficients (3.15), keeping in mind the goal of minimizing the threshold $\frac{K_0 + K_3 - 2K_1}{K_4}$. As a first benchmark, notice that if we choose the coefficients constant, we obtain the threshold scaling $\sim \frac{1}{\ell}$. Considering the numerator $K_0 + K_3 - 2K_1$, we complete a square to write $K_0 - 2K_1$ as a sum over $(c_{i+1} - c_i)^2$ which by taking a variational derivative naturally leads to c_i 's being an eigenfunction of the discrete 1D Laplacian, i.e., quadratic polynomials, cf. (3.15). Conveniently, this is a class of functions depending on only 3 parameters over which we can then optimize. The other term in the numerator, $K_3 = \left(\sum_{i=0}^{\ell-1} c_i d_i\right)^2$ can be viewed as a scalar product between the vector of d_i 's and the vector of c_i 's, so the Cauchy-Schwarz inequality says this is maximal if these vectors are collinear. Finally, regarding the choice of interpolation parameter $\lambda = \frac{2(\sqrt{2}-1)}{\ell}$, one can compute first that for $\lambda = \frac{C}{\ell}$ each term K_0, K_1, K_3 is a degree

10 polynomials in ℓ , with leading behavior $\frac{1}{900}\ell^8 + \frac{31}{1800}\ell^7$ independent of C . Thus $K_0 + K_3 - 2K_1$ is a degree 8 polynomial in ℓ . Since K_4 is $\frac{1}{\ell^2 + \ell}$ times a degree 12 polynomial in ℓ , this method indeed yields an $O(\frac{1}{\ell^2})$ scaling and it remains to choose C which we do by electing to minimize the leading term of the degree 8 polynomial $K_0 + K_3 - 2K_1$ in the numerator subject to the inequalities $K_3 \geq K_1, K_2$.

For small ℓ , namely $\ell \leq 9$, the leading term is no longer dominant and other choices of C (respectively t) yield appreciably smaller threshold. In this case, we instead rely on elementary optimization which yields the numbers displayed in Table 1.

3.7 Parameters in D dimensions

Proof of Theorem 2.2. Let $D \geq 2$. We apply Proposition 3.1 and analyze the formulae (3.3). Our goal is again to minimize $\frac{K_0 + K_3 - 2K_1}{K_4}$. With the exception of K_4 , all other expressions given above are equal to their 2D counterparts scaled by an additional factor of $\left(\sum_{i=0}^{\ell} d_i^2\right)^{D-2}$. K_4 is equal to its 2D counterpart scaled by a factor of $(\ell + 1)^{-(D-2)} \left(\sum_{i=0}^{\ell} d_i\right)^{2(D-2)}$. Thus, if we choose the coefficients c_i, d_i as in (3.15), we obtain from (3.20) that

$$\frac{K_0 + K_3 - 2K_1}{K_4} = \left(\frac{(\ell + 1) \sum_{i=0}^{\ell} d_i^2}{\left(\sum_{i=0}^{\ell} d_i\right)^2} \right)^{D-2} \left(\frac{36}{5\ell^2} + O\left(\frac{1}{\ell^3}\right) \right).$$

In order to derive error estimates, we note that both $(\ell + 1) \sum_{i=0}^{\ell} d_i^2$ and $\left(\sum_{i=0}^{\ell} d_i\right)^2$ are degree 6 polynomials in ℓ . By writing out these polynomials and using elementary estimates, we obtain the error estimate

$$\frac{(\ell + 1) \sum_{i=0}^{\ell} d_i^2}{\left(\sum_{i=0}^{\ell} d_i\right)^2} \leq \frac{6}{5}, \quad \ell \geq 10.$$

Similarly, one can show $\frac{K_4}{K_3} \geq \left(\frac{5}{6}\right)^D$, and so substituting in (3.14) we have

$$\gamma_L^{\text{per}} \geq \left(\frac{5}{6}\right)^D \left(\gamma_{\ell} - \left(\frac{6}{5}\right)^D \left(\frac{5}{\ell^2} + \frac{300}{\ell^3} \right) \right),$$

which proves Theorem 1. □

4 Proof of Theorem 2.5 on the honeycomb lattice

The proof follows the same general line of argumentation as the proof of Theorem 2.2 on the Euclidean lattice. The main difference is the definition of the weighting scheme which takes into account the local lattice geometry as described next.

4.1 Construction of weighted subsystem Hamiltonians

We let $c_0, \dots, c_{\ell-1}$ and d_0, \dots, d_{ℓ} be coefficients satisfying Requirements (i)-(iii) in Subsection 3.1 whose exact values will be determined later. We then define $W_{\mathcal{B}_{\ell}}$ analogously to (3.1) as the pointwise product of two simpler weighting schemes, now on the slanted grid B_{ℓ} , cf. Figure 1. To avoid introducing excessive notation for implementing this formally on the honeycomb lattice, we

summarize the honeycomb weighting scheme through Figure 5 which generalizes to arbitrary ℓ in an obvious way.

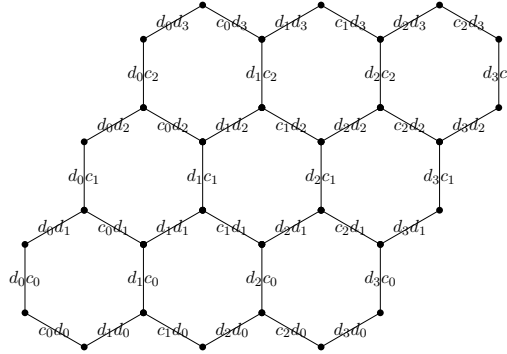


Figure 5: The weighted subsystem Hamiltonian $W_{\mathcal{B}_3}$ on slanted subgrids of the honeycomb lattice. Edges are labeled by their weights. This is the honeycomb analog of Figure 3.

As in the case of the square grid, the honeycomb weighting scheme displayed in Figure 5 is the pointwise product of the following two simpler weighting schemes.

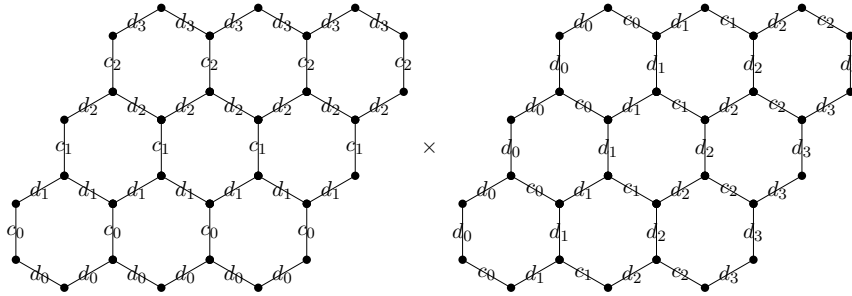


Figure 6: The weighted subsystem Hamiltonian $W_{\mathcal{B}_3}$ displayed in Figure 5 arises as the pointwise product of these two simpler weighting schemes; compare Figure 4.

In the next few subsections, we use the weighted subsystem Hamiltonians to prove an analog of Proposition 3.1 for the honeycomb lattice. Afterwards, in Subsections 4.4, we discuss how to choose the parameters c_i and d_i to optimize the relevant local gap threshold which will complete the proof of Theorem 2.5.

4.2 Expansion of the auxiliary operator

We let \mathcal{T}_L denote the set of possible translations of the plaquette \mathcal{B}_ℓ across \mathbb{H}_L , which we recall is the honeycomb lattice wrapped on an $L \times L$ torus. Given $t \in \mathcal{T}_L$, we write W_{B_t} for the correspondingly translated weighted Hamiltonian.

Combinatorial considerations parallel to those in Subsection 3.2 yield, after implementing the

symmetry requirement (ii) in Subsection 3.1,

$$\begin{aligned}
\sum_{t \in \mathcal{T}_L} W_{B_t}^2 = & \left(\left(\sum_{i=0}^{\ell} d_i^2 \right)^2 - 2d_0^4 \right) \sum_{\text{↘}} h_e \\
& + \left(\sum_{i=0}^{\ell} d_i^2 \right) \left(\sum_{i=0}^{\ell-1} c_i^2 \right) \left(\sum_{\text{↘}} h_e + \sum_{\text{⬇}} h_e \right) \\
& + \left(\sum_{i=0}^{\ell-1} d_i^2 \right) \left(\sum_{i=0}^{\ell-1} c_i d_i \right) \left(\sum_{\text{↘}} \{h_e, h_{e'}\} + \sum_{\text{↘}} \{h_e, h_{e'}\} \right) \\
& + \left(\sum_{i=0}^{\ell-1} c_i d_i \right)^2 \left(\sum_{\text{↘}} \{h_e, h_{e'}\} + \sum_{\text{↘}} \{h_e, h_{e'}\} \right) \\
& + \left(\left(\sum_{i=0}^{\ell} d_i^2 \right) \left(\sum_{i=0}^{\ell-1} c_i d_i \right) - c_0 d_0^3 \right) \left(\sum_{\text{↘}} \{h_e, h_{e'}\} + \sum_{\text{↘}} \{h_e, h_{e'}\} \right) \\
& + R,
\end{aligned} \tag{4.1}$$

Here, the various sums are taken over all edges with the indicated shape and R denotes the remaining sums over anticommutators corresponding to nonadjacent edges.

Notice that edges pointing in different directions do not appear with equal weights in the above expression. To remedy this, we consider the following direction-averaged auxiliary operator. We denote $W_{B_l}^{(0)} = W_{B_l}$ and, rotating it by 60 degrees clockwise, respectively counterclockwise, we obtain $W_{B_l}^{(1)}$ and $W_{B_l}^{(2)}$.

Summing formula (4.1) rotations and denoting $H_{\mathbb{H}_L} \equiv H_L$, we obtain

$$K_1 H_L^2 - \sum_{r=0}^2 \sum_{t \in \mathcal{T}_L} (W_{B_t}^{(r)})^2 \geq (K_1 - K_0) H_L \tag{4.2}$$

with the effective coefficients

$$\begin{aligned}
K_0 &= 2 \left(\sum_{i=0}^{\ell} d_i^2 \right) \left(\sum_{i=0}^{\ell-1} c_i^2 \right) + \left(\sum_{i=0}^{\ell} d_i^2 \right)^2 - 2d_0^4 \\
K_1 &= \left(\sum_{i=0}^{\ell} d_i^2 \right) \left(\sum_{i=0}^{\ell-1} c_i d_i \right) + \left(\sum_{i=0}^{\ell-1} d_i^2 \right) \left(\sum_{i=0}^{\ell-1} c_i d_i \right) + \left(\sum_{i=0}^{\ell-1} c_i d_i \right)^2 - c_0 d_0^3
\end{aligned}$$

assuming that K_1 is larger than all coefficients in the remainder R . Under our choice of coefficients specified below, this will indeed be the case.

4.3 Translation-invariant excited states

We have the following analog of Lemma 3.2.

Lemma 4.1. *There exists a normalized state $|\phi\rangle$ satisfying $H_{\mathbb{H}_L}|\phi\rangle = \gamma_L^{\text{per}}|\phi\rangle$ such that*

$$\langle \phi, (W_{B_t}^{(r)})^2 \phi \rangle \geq \gamma_\ell K_2 \langle \phi, W_{B_t}^{(r)} \phi \rangle, \quad t \in \mathcal{T}_L, \quad r = 0, 1, 2,$$

with

$$K_2 = \min \left\{ \frac{1}{\ell^2 + \ell} \left(\sum_{i=0}^{\ell} d_i \right) \left(\sum_{i=0}^{\ell-1} c_i \right), \frac{1}{\ell^2 + 2\ell - 1} \left(\left(\sum_{i=0}^{\ell} d_i \right)^2 - 2d_0^2 \right) \right\}.$$

Proof. This is a straightforward adaptation of the proof of Lemma 3.2. \square

We take the expectation of the operator inequality (4.2) in the state $|\phi\rangle$ and apply Lemma 4.1. This gives

$$\begin{aligned} K_1(\gamma_L^{\text{per}})^2 &\geq K_2 \gamma_\ell \left\langle \phi, \sum_{r=0}^2 \sum_{t \in \mathcal{T}_L} W_{B_t}^{(r)} \phi \right\rangle + (K_1 - K_0) \gamma_L^{\text{per}} \\ &= K_3 \gamma_\ell \gamma_L^{\text{per}} + (K_1 - K_0) \gamma_L^{\text{per}} \end{aligned}$$

where the second step follows from combinatorial considerations yielding the effective coefficient

$$K_3 = K_2 \left(2 \left(\sum_{i=0}^{\ell} d_i \right) \left(\sum_{i=0}^{\ell-1} c_i \right) + \left(\sum_{i=0}^{\ell} d_i \right)^2 - 2d_0^2 \right).$$

This proves the following general finite-size criterion on the honeycomb lattice

$$\gamma_L^{\text{per}} \geq \frac{K_3}{K_1} \left(\gamma_\ell - \frac{K_0 - K_1}{K_3} \right). \quad (4.3)$$

4.4 Coefficient choice and conclusion

Proof of Theorem 2.5. In view of (4.3), it remains to choose the coefficients c_i, d_i so as to optimize the threshold $t_\ell = \frac{K_0 - K_1}{K_3}$. Motivated by the considerations in the Euclidean situation, we set

$$\begin{aligned} c_j &= \ell + (\ell - 1)j - j^2 \\ d_j &= (1 - \lambda)(\ell + 1 + \ell j - j^2) + \lambda \left(\frac{(\ell + 2)^2}{4} \right) \end{aligned} \quad (4.4)$$

but this time we choose the tilting parameter $\lambda = -\frac{30}{11\ell}$. (This is obtained by setting $\lambda = \frac{C}{\ell}$ and optimizing the leading term of the resulting polynomial.) Note that the fact that $\lambda < 0$ is no obstruction since for large enough ℓ we still have positivity $d_j > 0$ as required.

Asymptotics. Under this choice of λ , we calculate the leading terms of the relevant ratios of polynomials and find

$$\begin{aligned} K_0 - K_1 &= \frac{19}{1980} \ell^8 + \frac{1076}{5445} \ell^7 + O(\ell^6) \\ K_3 &= \frac{1}{432} \ell^{10} + \frac{13}{264} \ell^9 + O(\ell^8). \end{aligned} \quad (4.5)$$

which yields a local gap threshold of the form

$$\frac{K_0 - K_1}{K_3} \geq \frac{228}{55\ell^2} + O\left(\frac{1}{\ell^3}\right),$$

which has the claimed leading asymptotics.

Error estimates. We can obtain an explicit, still rather crude error estimate by inspecting the coefficients of the polynomials. This yields for the local gap threshold

$$\frac{K_0 - K_1}{K_3} \leq \frac{228}{55\ell^2} + \frac{108}{\ell^3}$$

Finally, we obtain (2.4) in Theorem 2.5 from the bound $\frac{K_3}{K_1} \geq \frac{1}{2}$. The values displayed in Table 3 are obtained by explicit optimization of λ for small ℓ -values subject to the given constraints. \square

5 Proof of Theorem 2.7 on the triangular lattice

We follow the line of argumentation for Theorems 2.2 and 2.5. We focus on the key differences and omit other details.

To define the weighted subsystem Hamiltonians we use the weighting scheme depicted in Figure 7, which again can be viewed as arising from taking the products of edges from simpler Hamiltonians.

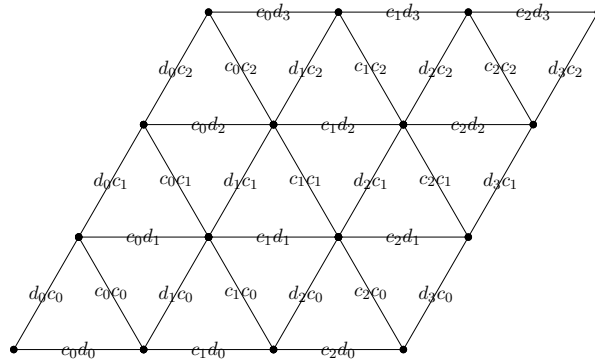


Figure 7: The weighted subsystem Hamiltonian $W_{\mathcal{B}_3}$ on the slanted subgrid of the triangular lattice. Edges are labeled by their weights. This is the triangular-lattice analog of Figure 3.

As in the honeycomb case, we define the appropriate auxiliary operator by summing over squares of translated and rotated copies of these weighted Hamiltonians, call them $\{W_{B_t}^{(0)}, W_{B_t}^{(1)}, W_{B_t}^{(2)}\}$, where t labels the possible translation in \mathcal{T}_L . We denote $H_{\mathbb{T}_L} \equiv H_L$. Combinatorial considerations yield

$$\sum_{t \in \mathcal{T}_L} \sum_{r=0,1,2} (W_{B_t}^{(r)})^2 = K_0 H_L + K_1 \sum_{\text{---}\text{---}} \{h_e, h_{e'}\} + K_2 \sum_{\text{---}\text{---}} \{h_e, h_{e'}\} + K_3 \sum_{\text{---}\text{---}} \{h_e, h_{e'}\} + R.$$

Here the sums are over all edge pairings of the associated shape (irrespective of orientation) and the term R contains anti-commutators over non-adjacent edges, which are positive semidefinite.

Moreover, we introduced the effective coefficients

$$\begin{aligned}
K_0 &= 2 \left(\sum_{i=0}^{\ell} d_i^2 \right) \left(\sum_{i=0}^{\ell-1} c_i^2 \right) + \left(\sum_{i=0}^{\ell-1} c_i^2 \right)^2 \\
K_1 &= 2 \left(\sum_{i=0}^{\ell} d_i^2 \right) \left(\sum_{i=0}^{\ell-2} c_i c_{i+1} \right) + \left(\sum_{i=0}^{\ell-2} c_i c_{i+1} \right)^2 \\
K_2 &= 2 \left(\sum_{i=0}^{\ell-1} c_i^2 \right) \left(\sum_{i=0}^{\ell-1} c_i d_i \right) + \left(\sum_{i=0}^{\ell-1} c_i d_i \right)^2 \\
K_3 &= 2 \left(\sum_{i=0}^{\ell-2} c_i c_{i+1} \right) \left(\sum_{i=0}^{\ell-1} c_i d_i \right) + \left(\sum_{i=0}^{\ell-1} c_i d_i \right)^2
\end{aligned}$$

Assuming that $K_2 \geq K_1, K_3$ and using the operator Cauchy-Schwarz inequality, we obtain

$$\begin{aligned}
K_2 H_L^2 - \sum_{r=0}^2 \sum_t (W_{B_t}^{(r)})^2 &\geq (K_2 - K_0) H_L + (K_2 - K_1) \sum_{\text{---}} \{h_e, h_{e'}\} + (K_2 - K_3) \sum_{\text{---}} \{h_e, h_{e'}\} \\
&\geq (K_2 - K_0) H_L - 2(K_2 - K_1) H_L - 4(K_2 - K_3) H_L \\
&= (2K_1 + 4K_3 - K_0 - 5K_2) H_L,
\end{aligned} \tag{5.1}$$

where in the first step we also discarded the terms in R using the assumption that the c_i, d_i are increasing up until their midpoints, and hence will have coefficients less than K_1, K_2, K_3 .

By adapting the proof of Lemma 3.2 to the triangular lattice, we obtain a normalized state $|\phi\rangle$ in the γ_L^{per} -eigenspace of H_L such that

$$\langle \phi | (W_{B_t}^{(r)})^2 | \phi \rangle \geq K_4 \gamma_\ell \langle \phi | W_{B_t}^{(r)} | \phi \rangle, \quad t \in \mathcal{T}_L, \quad r = 0, 1, 2, \tag{5.2}$$

with the new effective coefficient

$$K_4 = \min \left\{ \frac{1}{\ell^2 + \ell} \left(\sum_{i=0}^{\ell} d_i \right) \left(\sum_{i=0}^{\ell-1} c_i \right), \frac{1}{\ell^2} \left(\sum_{i=0}^{\ell-1} c_i \right)^2 \right\}.$$

Taking the expectation of (5.1) in the state $|\phi\rangle$, using (5.2), and calculating $\sum_{r=0}^2 \sum_t W_{B_t}^{(r)}$ yields

$$K_2 \gamma_L^{\text{per}} \geq K_5 \gamma_\ell + 2K_1 + 4K_3 - K_0 - 5K_2$$

with

$$K_5 = K_4 \left(2 \left(\sum_{i=0}^{\ell} d_i \right) \left(\sum_{i=0}^{\ell-1} c_i \right) + \left(\sum_{i=0}^{\ell-1} c_i \right)^2 \right).$$

This yields the general form of the finite-size criterion

$$\gamma_L^{\text{per}} \geq \frac{K_5}{K_2} \left(\gamma_\ell - \left(\frac{K_0 + 5K_2 - 2K_1 - 4K_3}{K_5} \right) \right)$$

It remains to choose the coefficients subject to the constraints (i)-(iii) and $K_2 \geq K_1, K_3$. Similarly to before, we take

$$\begin{aligned}
c_j &= \ell + (\ell - 1)j - j^2 \\
d_j &= (1 - \lambda)(\ell + 1 + \ell j - j^2) + \lambda \left(\frac{(\ell + 2)^2}{4} \right)
\end{aligned} \tag{5.3}$$

but now with $\lambda = \frac{-30+20\sqrt{5}}{11\ell}$, again a parameter chosen through optimizing the leading coefficient of the relevant polynomials.

With explicit error estimates for the subleading terms, we obtain

$$\gamma_L^{\text{per}} \geq \frac{1}{2} \left(\gamma_\ell - \left(\frac{144}{5\ell^2} + \frac{432}{\ell^3} \right) \right)$$

as claimed. To obtain the values in Table 4, we instead use (5.3) and optimize over λ for fixed ℓ subject to the given constraints. This completes the proof of Theorem 2.7. \square

References

- [1] H. Abdul-Rahman, M. Lemm, A. Lucia, B. Nachtergaele, and A. Young, *A class of two-dimensional AKLT models with a gap*, Analytic trends in mathematical physics, Contemp. Math. **741**, Amer. Math. Soc., Providence, RI 2020
- [2] I. Affleck, T. Kennedy, E.H. Lieb, and H. Tasaki, *Valence Bond Ground States in Isotropic Quantum Antiferromagnets*, Comm. Math. Phys. **115** (1988), no. 3, 477–528
- [3] A. Anshu, *Improved local spectral gap thresholds for lattices of finite size*, Phys. Rev. B **101** (2020), 165104
- [4] A. Anshu, I. Arad, and D. Gosset, *An area law for 2D frustration-free spin systems* (2021), preprint arXiv:2103.02492
- [5] I. Arad, Z. Landau, U. Vazirani, and T. Vidick, *Rigorous RG algorithms and area laws for low energy eigenstates in 1D*, Comm. Math. Phys. **356** (2018), no. 1, 65 – 105
- [6] S. Bachmann, S. Michalakis, B. Nachtergaele, and R. Sims, *Automorphic equivalence within gapped phases of quantum lattice systems*, Comm. Math. Phys. **309** (2012), no. 3, 835 – 871
- [7] T.S. Cubitt, D. Perez-Garcia, and M.M. Wolf, *Undecidability of the spectral gap*, Nature **528** (2015), no. 7581, 207–211
- [8] M. Fannes, B. Nachtergaele, R.F. Werner, *Finitely Correlated States on Quantum Spin Chains*, Commun. Math. Phys. **144** (1992), 443–490
- [9] D. Gosset and E. Mozgunov, *Local gap threshold for frustration-free spin systems*, J. Math. Phys. **57** (2016), 091901
- [10] M. B. Hastings, *An area law for one-dimensional quantum systems*, J. Stat. Mech. Theory Exp. **2007** (2007), no. 8, P08024
- [11] M. Hastings, *Lieb-Schultz-Mattis in higher dimensions*, Phys. Rev. B **69** (2004), 104431
- [12] S. Knabe, *Energy gaps and elementary excitations for certain VBS-quantum antiferromagnets*, J. Stat. Phys. **52** (1988), no. 3-4, 627 – 638
- [13] I. Jauslin and M. Lemm, *Random translation-invariant Hamiltonians and their spectral gaps*, preprint arXiv:2111.06433
- [14] M. Lemm, *Gaplessness is not generic for translation-invariant spin chains*, Phys. Rev. B **100** (2019), 035113
- [15] M. Lemm, *Finite-size criteria for spectral gaps in D-dimensional quantum spin systems*, Contemp. Math. **741**, Amer. Math. Soc., Providence, RI 2020

- [16] M. Lemm and E. Mozgunov, *Spectral gaps of frustration-free spin systems with boundary*, J. Math. Phys. **60** (2019) 051901
- [17] M. Lemm and B. Nachtergaele, *Gapped PVBS models for all species numbers and dimensions*, Rev. Math. Phys. **31** (2019), no. 9, 1950028
- [18] M. Lemm, A. Sandvik, and L. Wang, *Existence of a Spectral Gap in the Affleck-Kennedy-Lieb-Tasaki Model on the Hexagonal Lattice*, Phys. Rev. Lett. **124** (2020), 177204
- [19] B. Nachtergaele, *The spectral gap for some spin chains with discrete symmetry breaking*, Comm. Math. Phys. **175** (1996), no. 3, 565–606
- [20] B. Nachtergaele, and R. Sims, *Lieb-Robinson bounds and the exponential clustering theorem*, Comm. Math. Phys. **265** (2006), no. 1, 119 – 130
- [21] B. Nachtergaele, S. Warzel, and A. Young, *Spectral Gaps and Incompressibility in a $\nu = 1/3$ Fractional Quantum Hall System*, Comm. Math. Phys. **383** (2021), 1093–1149
- [22] N. Pomata, T.-C. Wei, *AKLT models on decorated square lattices are gapped*, Phys. Rev. B **100** (2019), 094429
- [23] N. Pomata, T.-C. Wei, *Demonstrating the Affleck-Kennedy-Lieb-Tasaki Spectral Gap on 2D Degree-3 Lattices*, Phys. Rev. Lett. **124** (2020), 177203
- [24] S. Spitzer and S. Starr, *Improved Bounds on the Spectral Gap above Frustration Free Ground States of Quantum Spin Chains*, Lett. Math. Phys. **63** (2003), 165–177
- [25] S. Warzel and A. Young, *A Bulk Spectral Gap in the Presence of Edge States for a Truncated Pseudopotential*, (2021), preprint arXiv:2108.10794